THREE-DIMENSIONAL TRACKING OF VARIOUS SIZED GLASS BEADS EJECTED FROM IMPACT CRATER. H. Okawa[1], M. Arakawa[1], M. Yasui[1], S. Hasegawa[2], Y. Yokota[1], Y. Yamamoto[1], [1]Graduate School of Science, Kobe University, [2] Japan Aerospace Exploration Agency, Institute of Space and Astronautical Science.

Introduction: The ejection process during the crater formation is important to consider the resurfacing process on solid bodies, and there are many studies related to the ejection process. For example, the ejecta velocity distribution is known to be well described by the following π-scaling theory [1]:

$$\frac{v_0}{\sqrt{gR}} = k_2 \left(\frac{r_0}{R}\right)^{-\frac{1}{\mu}}, \quad (1)$$

where v_0 is the ejection velocity of the ejecta particle, r_0 is the distance between the initial positions of the ejected particles and the impact point of the projectile, R is the crater radius, and g is the gravitational acceleration. This scaling law was constructed based on the experimental results for the targets composed of homogeneous sized regolith particles and the scaling law does not include the effect of the target particle size. In addition, previous cratering experiments showed that an axisymmetric cone-like ejecta curtain was developed on granular targets with a uniform particle size. On the other hand, recent asteroid explorations revealed that the boulders on the asteroid surface had a size frequency distribution in a wide range of the boulder size [2][3]. The impact cratering experiment by Hayabusa2 spacecraft, which actually observed the crater formation process on the asteroid surface by DCAM3, resulted in the formation of the asymmetric and heterogeneous ejecta curtain [4]. The formation mechanism of the asymmetric and heterogeneous ejecta curtain can be assumed related to the ejecta velocity distribution depending on the particle sizes so far.

In this study, we carried out impact cratering experiments on granular particles with various sizes to investigate the ejecta velocity distribution, and we then discussed the effect of ejecta particle size on the π-scaling theory for ejection velocity distribution. Moreover, we estimated the maximum size of the boulder which could be ejected from the final crater.

Experimental methods: We conducted the impact experiments by using a one-stage vertical gas gun at Kobe University, and a two-stage vertical gas gun at ISAS. These guns have different impact velocity ranges: the impact velocity, v_i, ranged from 105 to 208 m s^{-1} at Kobe University (relatively low velocity) while the v_i ranged from 1.2 to 4.4 km s^{-1} at ISAS (relatively high velocity). At Kobe University, we used spherical projectiles made of nylon, glass, alumina, titanium, zirconia, and iron with the diameter of 3 mm. The target chamber was evacuated below 10^3 Pa before the shot. At ISAS, we used spherical projectiles made of aluminum, titanium, iron, and copper with the diameter of 1 or 2 mm. The target chamber was evacuated from 1.5 to 3.5 Pa.

We used two types of targets, "heterogeneous target" and "homogeneous target". Heterogeneous target is a mixture of spherical glass beads with the size of 0.1, 1, 3, and 10 mm. The angle of repose was measured to be 22 ± 2º. The grain density of the bead was 2.5 g cm^{-3} and the calculated bulk density of the target was 1.97 g cm^{-3}. Homogeneous target is composed of glass beads with the median grain size of about 0.1 mm. The angle of repose was 23 ± 1º and the bulk density was 1.42 g cm^{-3}.

The analytical method to determine 3D traces of ejected beads is described as follows. First, for the calibration, we recorded a rectangular parallelepiped reference (30 cm × 30 cm × 40 cm) by two cameras and determined the spatial coordinate of the target in the chamber. These two cameras were set at in the top and front of the chamber. Next, we conducted an impact experiment without the reference box and recorded the ejecta curtain by the two synchronized cameras. In order to identify an individual bead on their images, colored glass beads (3, 5, 10, 18 mm in the diameter) were set on the target surface at different positions from the impact point. Finally, we tracked the colored beads on each image to reconstruct the trace, and then each bead position in the three-dimensional coordinate system was determined based on the calibration.

We assumed that ejecta particles moved at a constant velocity in the horizontal direction relative to the target surface while they were accelerated in a vertical direction by the earth's gravity of 9.8 m s^{-2}: they had parabola trajectories. Moreover, we analyzed the three-dimensional ejection vector using the trajectory of the ejected beads obtained by the above method, and determined the ejection angle and the azimuth angle as well as the ejection velocity with respect to the ejection position (Fig. 1).

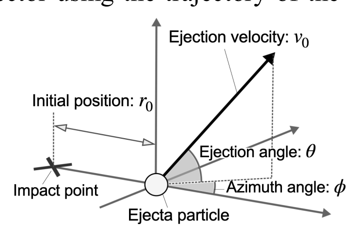

Fig. 1 The three-dimensional ejection vector of a particle.

Results: In our experiments, we observed an axisymmetric but heterogeneous ejecta curtain for all shots. First of all, we confirmed that the above assumptions were valid for the ejecta movement, then we succeeded to obtain the three-dimensional trajectories of the ejecta particles in the heterogeneous ejecta curtain. The obtained ejection vectors showed us that they depended on the target type. For the heterogeneous targets, the ejection angle and the azimuth angle widely varied in the range of 30–62º and 0–65º, respectively while their ranges were narrower for the homogeneous targets: They were 51–60º and 0–13º, respectively.

Fig. 2a shows the relationship between the normalized ejection velocity of the colored beads, $v_0/\sqrt{gR}$, and their ejection positions normalized by the crater radius, r_0/R for the homogeneous targets. The r_0 shows the distance from the impact point to the center of the particle as shown in Fig. 3. Although the relationship almost follows Eq. (1), we found that the ejection velocity became lower when the bead size was larger. This means that the ejecta velocity distribution would depend on the particle size. Therefore, we recalculated the relationship by using the ejection position, r_0', which means the distance from the impact point to the outside edge of the bead, instead of the r_0. As a result, the normalized ejection velocity was well scaled by r_0', and it did not depend on the bead size no more. This improved relationship could be approximated by one exponential function. The fitted equation by using the Eq. (1) and the r_0' instead of r_0 was obtained to be $v_0/\sqrt{gR} = 0.75(r_0'/R)^{-1/0.60}$.

On the other hand, the ejecta velocity distribution for the heterogeneous targets were scattered and we could not find the dependence on the particle size.

Discussions: We constructed a model to describe the ejection velocity of large particles with the size much larger than the surrounding particles and compared our model with the experimental results. A large particle on the target surface is expected to be ejected by push of the subsurface materials during the excavation. Therefore, the ejection velocity of a large particle could be controlled by the average velocity of the excavated material with the volume V in Fig. 3. The average velocity $\bar{v}$ can be obtained by using the V and the momentum of the excavated region calculated from the Z-model [5] and the ejecta velocity scaling law [1]. The $\bar{v}$ normalized by $\sqrt{gR}$ can be obtained by the following equation:

$$\frac{\bar{v}}{\sqrt{gR}} = \frac{3k_2\mu}{3\mu-1}\cdot\frac{(x_2/R)^{3-1/\mu}-(x_1/R)^{3-1/\mu}}{(x_2/R)^3-(x_1/R)^3} \qquad (2)$$

In this calculation, our experimental results are found to be well explained by the model when we set the x_1 in Fig. 3 as $r_0 - a$ and the x_2 as $r_0 + 3a$. The colored lines in Fig. 2 indicate the Eq. (2) calculated by using the ejected bead radius a, and they are consistent with the experimental result for each ejected bead radius.

We applied our new scaling law for the ejecta velocity distribution applicable to large particles to calculate the maximum size of the boulder which can be ejected outside the final crater. As a result, we found that the boulders with the radius larger than 0.3 times the crater radius could not be ejected outside the final crater, that is, they could land inside the crater. Therefore, we propose that the maximum boulder radius ejected outside the final crater is smaller than 0.3 times the crater radius.

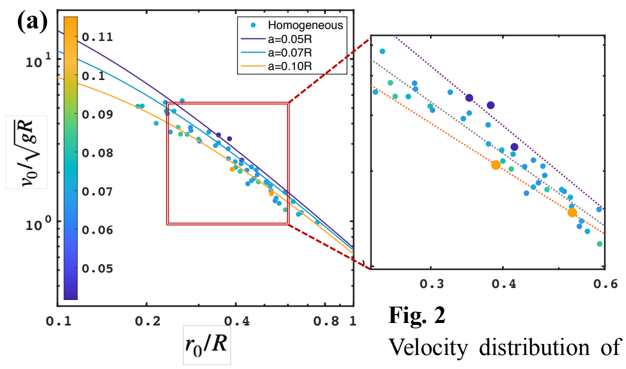

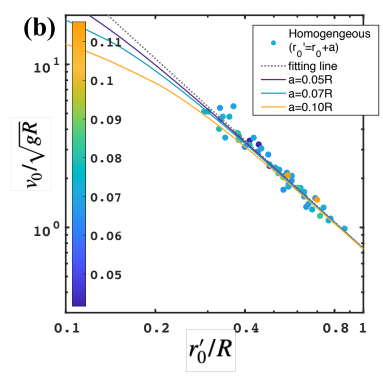

Fig. 2 Velocity distribution of various sized ejected beads set on a homogeneous target. The initial position of the beads was described by, (a) r_0 and (b) r_0'. The plot color shows the ejected bead radius normalized by the crater radius. The figure on the right of panel (a) shows the enlarged one of the box in the panel (a).

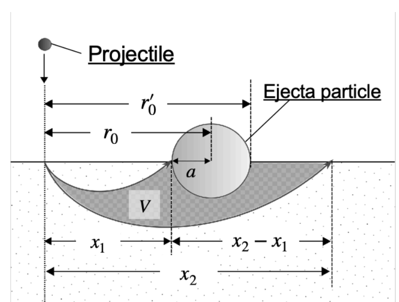

Fig. 3 Parameters related to the ejection point and the excavation region.

References: [1] Housen, K. R. and Holsapple, K. A. (2011) *Icarus* 211, 856-875. [2] Sugita, S. et al. (2019) *Science* 364, aaw0422. [3] Michikami, T. et al. (2019) *Icarus* 331, 179-191. [4] Arakawa, M. et al. (2020) *Science* 368, 67–71. [5] Maxwell, D. E. (1977) Pergamon, NY, pp. 1003–1008.